Transition Spectra in the Vibrational Quasicontinuum of Polyatomic Molecules: Raman Spectra of Highly Excited UF_6 Molecules†

A. A. Kosterev, A. A. Makarov, A. L. Malinovsky, I. Yu. Petrova, E. A. Ryabov, and V. S. Letokhov*

Institute of Spectroscopy, Russian Academy of Sciences, 142190 Troitsk, Moscow Region, Russia

Received: March 10, 2000; In Final Form: June 6, 2000

Spontaneous Raman spectra of highly excited UF_6 molecules in the vicinity of the mode ν_1 are studied. The spectra measured are interpreted within the framework of the model suggested, which presumes the dominant role of statistical inhomogeneous broadening in the formation of transition spectra in the vibrational quasicontinuum. A good agreement is obtained between the theoretical and experimental spectra of UF_6 molecules heated to $T_{vib} = 1320$ K. The relationships are found between the vibrational energy of the UF_6 molecule and the main parameters of its Raman transitions in the neighborhood of the frequency of the mode ν_1, such as the intensity, width, and maximum positions of their profiles.

1. Introduction

The object of study in the traditional vibrational spectroscopy of molecules is usually their vibrational−rotational states near the bottom of their potential surface. The development of laser spectroscopy techniques made it possible to launch studies into highly excited states in polyatomic molecules, at energies up to their dissociation limit, in the region of the so-called vibrational quasicontinuum (QC). Interest in this region of the energy spectrum is largely associated with intramolecular dynamics investigations (for references, see, e.g., refs 1−3), as well as with the development of laser methods to monitor and control the dynamics of chemical reactions.[4,5] It should be noted that subject to study in the majority of cases are *ground state* → *QC* transitions. A review of these works can be found in ref 6 (see also ref 7). For various reasons, experimental difficulties included, transitions *between quasicontinuum states* (QC → QC transitions) have been studied much less. (A brief review of these works can be found in ref 8.) At the same time, it is exactly the QC → QC transitions that prove to be decisive in many cases, such as the IR fluorescence and Raman spectra of highly excited molecules, and also the IR absorption of molecules, including their multiple-photon excitation (MPE).

This work continues the series of our publications[8−12] devoted to our investigations of QC → QC transitions. The profile shape and width of vibrational transitions between quasicontinuum states are mainly governed by two factors: the *homogeneous broadening* and *statistical inhomogeneous broadening* (SIB). The first type of broadening is associated with the IVR processes occurring in the molecule. The second type is due to the dispersion of the transition frequencies from a given mixed vibrational state which is contributed to by a large number of harmonic states with various combinations of the occupation numbers in the modes. The anharmonic transition frequency shift of any such combination being different from those of the other combinations leads to a statistical inhomogeneous broadening of the spectrum (for details, see ref 8 and references therein). The objects of our studies were XY_6-type molecules. In our work reported in ref 8, we developed an approach allowing the main parameters, such as the intensity, shape, and maximum positions of QC → QC transition profiles, to be calculated on the basis of the values of the fundamental frequencies ν_i and anharmonicity constants x_{ij} in the approximation where the dominant part was played by the SIB effect. Using this approximation, we calculated in ref 8 the above parameters for transitions in the vicinity of the frequencies of the modes ν_1 and ν_3 in SF_6, as well as for the mode ν_3 in WF_6. We also demonstrated that SIB resulted in the transition profiles acquiring a Gaussian shape. The correctness of this approach was verified in ref 9 by comparing experimental and theoretical Raman spectra near the frequency of the mode ν_1 of highly excited SF_6 molecules. The conclusion was drawn in this work that, in the case of the mode ν_1 in SF_6, it was exactly SIB that mainly contributed to the formation of the QC → QC transition spectrum, the contribution from homogeneous broadening being considerably less. This conclusion as to the dominant role of the SIB effect in SF_6 was also shown to hold true for the mode ν_3 in refs 10 and 11 where subject to study was the IR MP absorption spectrum of this molecule. Moreover, by comparing experimental and theoretical IR MP spectra, we managed to determine the half-width γ_L of the homogeneous Lorentzian profile in a wide range of vibrational energies. Note also that the method developed for calculating the parameters of QC → QC transitions allowed the authors of ref 12 to reconstruct, on the basis of experimentally measured Raman spectra, the form of the vibrational distribution function formed as a result of the IR MPE of SF_6.

The present work is devoted to studies into the spectra of highly excited UF_6 molecules. Like the other XY_6-type molecules, UF_6 features two very strong vibrations, namely ν_1 and ν_3, active in Raman scattering and IR absorption, respectively. In our experiments, UF_6 molecules were "heated" to various vibrational temperatures by way of their IR MP excitation via the ν_3 vibration. Thereafter their spontaneous Raman scattering (SRS) spectra in the vicinity of the frequency of the mode ν_1 were measured under equilibrium vibrational distribution conditions. The Raman spectra thus obtained were compared with

† Part of the special issue "C. Bradley Moore Festschrift".

* Corresponding author: FAX: (+7−095)334 08 86. E-mail: letokhov@isan.troitsk.ru.

10.1021/jp000928d CCC: $19.00
Published on Web 08/10/2000

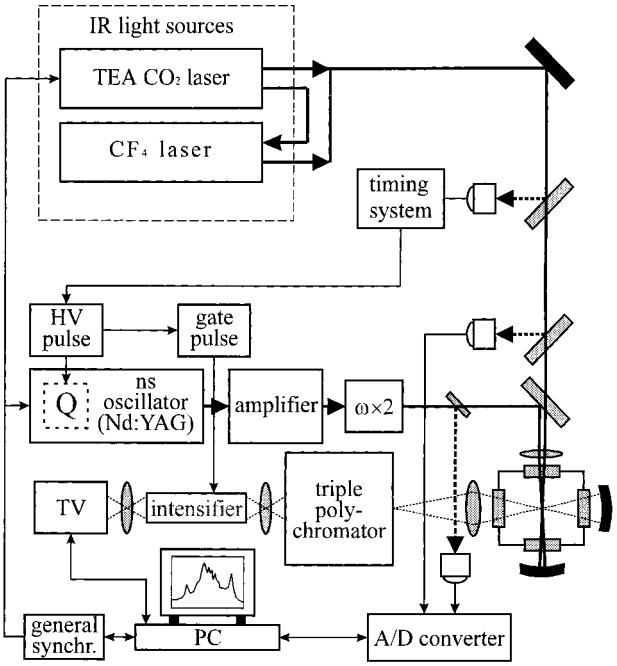

Figure 1. Schematic diagram of the experimental setup.

their theoretical counterparts calculated on the basis of the model approach developed. The results obtained are presented below.

2. Experiment

2.1. Measurement Method. The measurement procedure used in this work was in many ways similar to the one used earlier in the experiments[9] with SF_6. The experimental setup is shown schematically in Figure 1. The UF_6 molecules in this experiment were excited by means of a pulsed CF_4 laser optically pumped by a TEA CO_2 laser.[13] The output frequency of the latter laser was stabilized with a cw CO_2 laser. The used radiation frequency of the CF_4 laser, $\omega = 615.3$ cm^{-1}, falls within the absorption band of the ν_3 vibration (627.7 cm^{-1}) in UF_6. The duration of the IR pulse, τ_{pump}, was around 80 ns (fwhm) and no more than 180−200 ns (full width). The CF_4 laser radiation was focused by means of a cylindrical KBr lens into the cell containing the molecular gas under study. The waist width amounted to some 0.4 mm (fwhm). The IR radiation fluence Φ_{IR} in the waist could reach 1 J/cm^2. The Raman probing of the molecules under study was effected by means of the second-harmonic radiation from a Nd^{3+}:YAG laser ($\tau_{probe} \simeq 7$ ns, $E_{pulse} \simeq 30$ mJ). The probe pulse passed through the waist of the cylindrical lens at right angles to the propagation direction of the IR pulse (and parallel with the entrance slit of a polychromator) some time τ_d after the latter. The radiation scattered from the waist of the probe beam was collected by means of a suitable optical system and focused onto the entrance slit of a triple polychromator. The radiation at the exit from the polychromator was detected with a multichannel optical detector. The detector consisted of a vidicon TV camera and an image intensifier gated in step with the probe pulse. All spectral measurements were taken in the photon counting mode.

We measured not only the Raman signal, but also the energies of the IR and probe pulses. This allowed us to sort out the spectral signals, i.e., to add together the images registered by the vidicon camera after each laser shot in an appropriate computer memory array (up to 6 arrays) and also to sum up the laser shots and the laser pulse energy values for each array.

The repetition rate of the laser pulses and of the entire data acquisition cycle amounted to 6.25 Hz.

The pressure p of the UF_6 gas in the sample cell usually came to 0.5 Torr, which provided for practically collision-free IR MP excitation conditions at the IR pulse duration used.

In view of the high chemical activity of UF_6, a number of measures were taken prior to and during the course of the experiment to prevent any uncontrolled changes in the gas concentration in the sample cell. First of all, the cell was preliminarily passivated by exposing it to UF_6 at a pressure of around 20 Torr for 30−40 min. As shown by our measurements of the SRS signal after passivation, the rate of reduction of the UF_6 gas concentration in the cell amounted to some 7% per hour. Proceeding from this result, the substance under study in the cell was changed every 30−40 min in the course of regular measurements. Besides, the IR radiation fluence Φ_{IR} did not, as a rule, exceed the IR MP dissociation threshold.

2.2. Measurement Results. As already noted, we chose for spectral measurement purposes the strongest Raman-active mode ν_1 (667.2 cm^{-1}) of UF_6, for which it is only the Q-branch transitions that are allowed by the selection rules. In this work, we present the results of measuring the "equilibrium" spectra of the excited molecules in the vicinity of the frequency of this mode. These were obtained in conditions where a Boltzmann vibrational distribution must have been established after the passage of the IR pulse. As in the case of SF_6, the choice of the "equilibrium" spectra was dictated by the fact that to correctly compare between experimental and theoretical spectra, it is necessary to know the exact form of the population distribution function. The Boltzmann distribution characterizes the population at equilibrium.

The "equilibrium" spectra were usually measured at one of two values of the delay time between the pump and probe pulses, either $\tau_d = 2$ μs or $\tau_d = 4$ μs, so that the parameter $p\tau_d$ amounted to 1 μs·Torr or 2 μs·Torr, respectively. According to ref 14, the characteristic time it takes for vibrational equilibrium to be established in UF_6 as a result of collisions is $p\tau(UF_6-UF_6) = 0.5$ μs·Torr. We, therefore, believe that a Botltzmann distribution with a characteristic vibrational temperature of T_{vib} must assuredly be established by the moment the probe pulse arrives, at least at the longest of the delay times τ_d selected. This assumption was indirectly shown to be true by the fact that the shape of the spectra corresponding to one and the same Φ_{IR} values remained unchanged when the delay time τ_d was varied over the above limits. At the same time, as distinct from the measurements taken earlier with the SF_6 molecule,[15] the spectrum-integrated SRS signal diminished with variation of τ_d perceptibly. Simple estimates show that the reduction of the signal mentioned above cannot be due to the redistribution of energy from the mode ν_1 being observed in this molecule into its other modes on account of the V−V′ relaxation process. It is our opinion that this effect is mainly associated with the change of the number of particles in the volume being probed. Estimates show that at the $p\tau_d$ values selected there can already occur a noticeable diffusion of the particles from the excitation region. What is more, as follows from ref 14, the V−T/R relaxation process in UF_6 proceed much faster than in SF_6, which may additionally contribute to the rate of "departure"of the particles.

Figure 2 presents "equilibrium" Stokes spectra in the region of the frequency of the mode ν_1 in UF_6. The spectrum of Figure 2a was obtained prior to the passage of the pump pulse and corresponded to room temperature ($T = 299$ K). The somewhat asymmetric shape of the spectrum is due to the presence of a large number of hot bands, only around 0.4% of the molecules being in their ground state at room temperature. Even a relatively

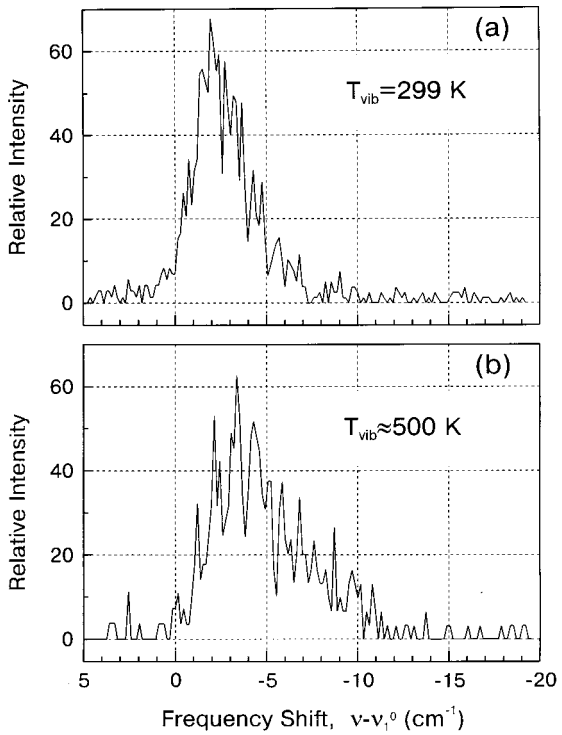

Figure 2. Stokes Raman spectra in the vicinity of the frequency of the mode ν_1 in UF_6 at $T_{vib} = 299$ K (a) and $T_{vib} \simeq 500$ K (b). $\tau_d = 2$ μs, $p = 0.5$ Torr.

low heating of the molecules as a result of their IR MP excitation causes a substantial modification of the spectrum: it shifts toward the "red" side and broadens. This can clearly be seen in Figure 2b which presents the Raman spectrum of UF_6 at $T_{vib} \simeq$ 500 K. (Note that the "jagged" character of the spectrum is mainly associated with the photon counting statistics in the different channels of the multichannel detector.)

The subsequent and more thorough measurements of UF_6 spectra were taken in the anti-Stokes region because the parasitic noise level here is much lower. The spectra were measured at various values of the CF_4-laser fluence Φ, which were selected so as to cover the maximum possible variation range of the vibrational temperature T_{vib} and avoid at the same time the dissociation of the UF_6 molecules. Some of the "equilibrium" spectra thus obtained are shown in Figure 3. For the reasons discussed above, it proved impossible in the case of UF_6 to determine T_{vib} on the basis of the spectrum-integrated Raman signal as in the case of SF_6 (for details, see ref 9). Therefore, the T_{vib} values indicated on the spectra presented in Figure 3 were obtained on the basis of spectral measurements (see below). The results of Figure 3 show that even when the UF_6 molecules are heated to a fairly high temperature (to $T_{vib} \simeq 1320$ K), their Raman spectra remain quite localized in the neighborhood of the frequency of the mode ν_1. At the same time, as one might expect, the spectra of the excited states of the molecules get shifted toward the long-wavelength region because of the anharmonicity of their vibrations, this shift increasing with the increasing temperature T_{vib}. Simultaneously there takes place the broadening of the spectra. The theoretical analysis of the results obtained is presented below.

3. Comparison between Experimental and Theoretical Spectra

When processing the SRS spectra obtained, we generally adhered to the approach that we developed and used successfully

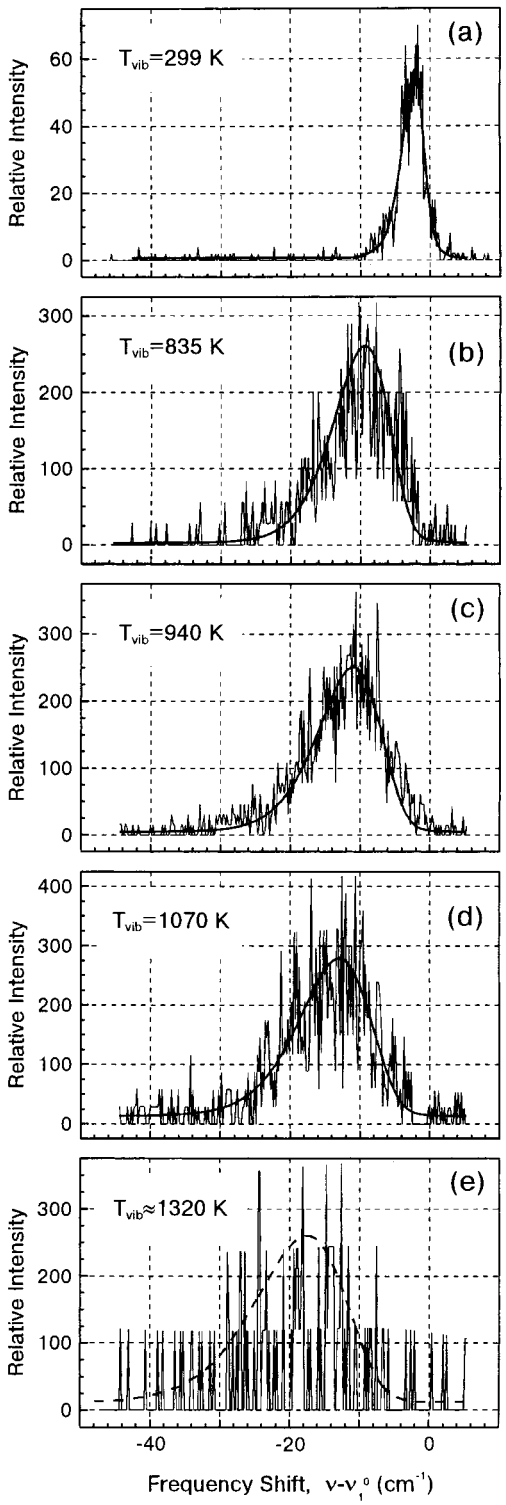

Figure 3. Anti-Stokes Raman spectra of excited UF_6 molecules at various vibrational temperatures. $\tau_d = 2$ μs, $p = 0.5$ Torr. The smooth solid curves − model calculations. Fluence Φ_{IR}: (a) 0.0 J/cm^2; (b) 0.12 J/cm^2; (c) 0.21 J/cm^2; (d) 0.31 J/cm^2; (e) ≥ 0.44 J/cm^2.

for SF_6 in refs 8, 16, 21. The main principles at the root of the model developed are most fully described in ref 21. Here we will restrict ourselves only to the principal points necessary for the exposition of the essence of the problem.

It has been demonstrated in ref 16 that to adequately describe the SRS spectrum of an ensemble of highly excited molecules it is quite sufficient to take into consideration a limited sample of states equidistant in E_{vib} with due regard for their statistical

properties. In that case, the expression for the model spectrum may be written in the form (the sign ⊗ here stands for a convolution of functions)

$$MS(\nu;T_{\mathrm{vib}}) = V\sum_k F(E_{\mathrm{vib}}^{(k)})\,\Psi(\nu, E_{\mathrm{vib}}^{(k)}) \otimes \Phi_{\mathrm{rot}} \otimes \Phi_{\mathrm{sf}} \quad (1)$$

where V is the normalization coefficient.

In the above expression, $F(E_{\mathrm{vib}})$ is the population distribution function; proceeding from what has been said in the preceding section, it must be a Boltzmannian:

$$F(E_{\mathrm{vib}}) = \rho(E_{\mathrm{vib}})\exp(-E_{\mathrm{vib}}/(kT_{\mathrm{vib}})) \quad (2)$$

where $\rho(E_{\mathrm{vib}})$ is the density of vibrational states. Φ_{rot} is the rotational band shape for which one can obtain the following expression:

$$\Phi_{\mathrm{rot}}(\nu) = \left(1 + 4\frac{\nu}{\alpha_1}\right)\exp\left(-\frac{\nu B}{\alpha_1 T_{\mathrm{rot}}}\right)$$

for $\nu \le 0$, and

$$\Phi_{\mathrm{rot}}(\nu) = 0 \quad (3)$$

for $\nu > 0$, with the parameters $B = 5.567 \times 10^{-2}$ cm^{-1} and $\alpha_1 = -1.2 \times 10^{-4}$ cm^{-1}.[17] The rotational temperature T_{rot} in eq 3 was taken in our calculations to be equal to $T_{\mathrm{rot}} = 299$ K. Actually, due to a much faster $V - T/R$ rate for UF_6, as compared with SF_6, the rotational degrees of freedom may be also partially heated at $p\tau_d = 2$ μs·Torr. But, the spectral calculations show that this possible heating produces the minor effect even in the limiting case of $T_{\mathrm{rot}} = T_{\mathrm{vib}}$. In eq 1, Φ_{sf} is the spread function of our apparatus, which was found to be the convolution of a Lorentzian and a Gaussian function with the parameters $\gamma_{\mathrm{sf}} = 0.738$ cm^{-1} and $\sigma_{\mathrm{sf}} = 0.722$ cm^{-1}, respectively. The function $\Psi(\nu, E_{\mathrm{vib}})$ describes the band profile and intensity of transitions from the state with the given energy E_{vib}.

The method developed in ref 8 to calculate the shape and parameters of QC → QC transitions holds true under the assumption of the dominant role of statistical inhomogeneous broadening. The subsequent measurements[9−11] showed that this approximation was valid for SF_6 and that the relative role of homogeneous broadening was indeed small, at least for one-photon transitions. For this reason, when modeling the spectra of highly excited molecules in this work, we also used the SIB approximation.

The function $\Psi(\nu)$ was calculated by the method described below. First we determined in the harmonic approximation the energies of all *regular states* in some energy interval $\pm\Delta E$ (ΔE was varied from 50 cm^{-1} at $E_{\mathrm{vib}} = 1200$ cm^{-1} to 0.5 cm^{-1} at $E_{\mathrm{vib}} = 24600$ cm^{-1}) in the vicinity of some *mixed state* with a given energy E_{vib} by directly searching through all of the occupation numbers n_i involved:

$$E_j = \sum n_i\nu_i \qquad E_j \in [E_{\mathrm{vib}} - \Delta E, E_{\mathrm{vib}} + \Delta E\,]$$

(As shown by the analysis made in ref 9 for SF_6, the inclusion of anharmonic terms into the expression for the energy of regular states only gives rise to small corrections known to be much inferior to the experimental errors inherent in the spectra measured. Besides, the entire matrix of the anharmonicity constants x_{ij} is not known.) Next we found all of the possible transitions from these states that involved a unit decrease of the occupation number n_1 in the mode ν_1, i.e., $n_1 \rightarrow n_1 - 1$ (anti-Stokes transitions). In accordance with the approximation used, the intensity of these transitions was taken to be proportional to n_1:

$$I_{\mathrm{aS}} \sim n_1$$

Because of anharmonicity, the frequency of these transitions must be shifted with respect to the frequency ν_1^0 of the fundamental transition:

$$|1, 0, 0, 0, 0, 0\rangle \rightarrow |0, 0, 0, 0, 0, 0\rangle.$$

The magnitude of this shift was computed by the formula

$$\Delta\nu_1 = 2x_{11}(n_1 - 1) + \sum_{i\neq 1} x_{1i}n_i \quad (4)$$

The values of the fundamental frequencies ν_i and anharmonicity constants x_{ij} used in these computations are listed in Table 1.

Thereafter, we convolved the histogram thus obtained with the Gaussian component of our spread function. Figure 4 presents the band profiles $I_\nu = I_\nu(\Delta\nu)$ for the following three values of E_{vib}: 5000, 10 000, and 20 000 cm^{-1}. It can be seen that as E_{vib} is increased, the maximum $\Delta\nu_{\max}$ of the profile shifts

TABLE 1: UF_6 Vibrational Frequencies and Anharmonic Constants Used to Calculate the Transition Profiles of Figure 4

	mode (i)					
	1	2	3	4	5	6
ν_i (cm^{-1})	667.2[a]	533[a]	627.7[b]	189[a]	200[a]	144[a]
x_{1i} (cm^{-1})	−0.3[c]	−1.8[a]	−1.6[a]	−0.2[a]	−0.25[a]	−0.1[a]

[a] Taken from ref 17. [b] Taken from ref 18. [c] Taken from ref 19.

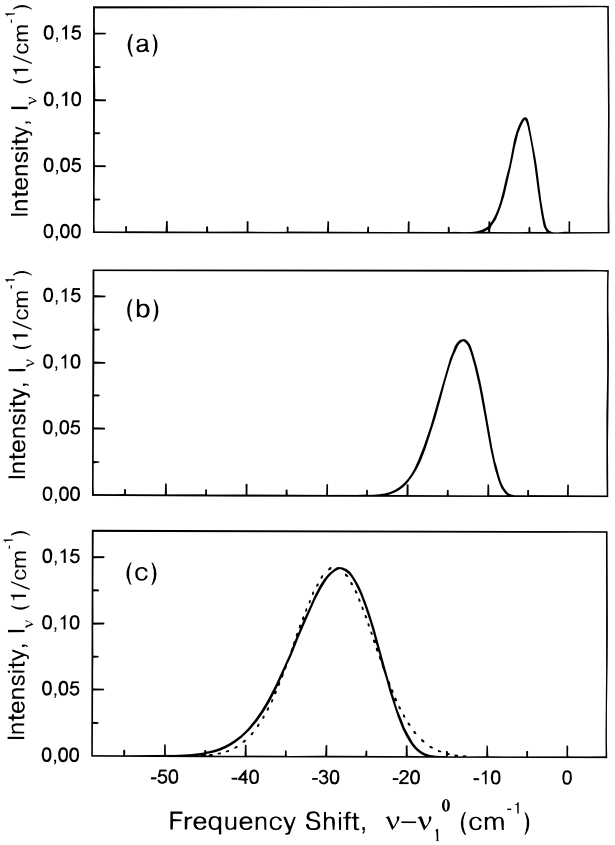

Figure 4. Theoretical band profiles (solid curves) of anti-Stokes transitions in the vicinity of the frequency of the mode ν_1 in UF_6 at various initial vibrational energies E_{vib}: (a) 5000 cm^{-1}; (b) 10 000 cm^{-1}; (c) 20 000 cm^{-1}. The dashed curve is the best fit by a Gaussian function.

toward the long-wavelength side and its width materially broadens to reach sufficiently high values as a result of the SIB effect. To illustrate, at $E_{vib} = 20\,000$ cm^{-1} the profile half-width (standard deviation) σ_0 amounts to 4.96 cm^{-1}.

On the basis of our calculations, we obtained the following approximate expressions for the shift of the maximum $\Delta\nu_{max}$ of the profile (reckoned from the position of the unexcited transition frequency ν_1^0) and its half-width σ_0 as a function of the vibrational energy E_{vib} (in cm^{-1}) at $E_{vib} \geq 2000$ cm^{-1}:

$$\Delta\nu_{max}(E_{vib}) = 1.67 - (1.56 \times 10^{-3})\cdot E_{vib}$$

$$\sigma_0(E_{vib}) = 0.337 + (0.231 \times 10^{-3})\cdot E_{vib}$$

The relationship between the spectrum-integrated transition intensity I_0 (in units of intensity of the transition $0 \rightarrow 1$) and E_{vib} may be written in the form

$$I_0\,(E_{vib}) = -0.15 + (0.0963 \times 10^{-3})\cdot E_{vib}$$

It should, however, be noted that in contrast to SF_6 the shape of the band profile features a perceptible asymmetry. This is evident from Figure 4c, which also shows the best fit of the profile (the dashed curve) by a Gaussian function. Our analysis has shown that this asymmetry is caused by the substantial deviation of the values of the constants x_{12} and x_{13} from those of the other constants (see Table 1). This difference in SF_6 is much smaller (see Table 1 in ref 9), so that the resultant profile is much more symmetric and can be well approximated by a Gaussian function. To describe the actual profile shape in this work we used the "skew" Gaussian function

$$\Psi(\nu) = A \exp\left[\frac{(\nu - \nu')^2}{2\sigma^2}\right] \exp[k_1 \exp(k_2(\nu - \nu')] \qquad (5)$$

where A, σ, ν', k_1, and k_2 are variable parameters ($k_1 < 0$, $k_2 > 0$). Note that the parameters σ and ν' in the above expression are generally other than the half-width and the maximum of the profile under consideration, as is the case with the "pure" Gaussian, and approach their "true" values only as $k_1 \rightarrow 0$.

In finding the numerical values of all the above parameters, we adhered to the so-called least-squares tenet, i.e., we tried to minimize the quantity χ^2 defined in the general case by the expression

$$\chi^2 = \sum_i [D(x_i) - M(x_i;\{p\})]^2 \qquad (6)$$

where $D(x_i)$ is the set of data points to be approximated, $M(x_i;\{p\})$ is the model fitting function. In our case, $D(x) = I_\nu(\nu)$ and $M(x_i;\{p\}) = \Psi(\nu; A, \sigma, \nu', k_1, k_2)$. Using eq 5, one can very well describe the band profiles obtained. To illustrate, if in the case of Figure 4c the quantity χ^2 defined by eq 6 amounts to 8.06×10^{-3} cm^2 when using the pure Gaussian function for fitting purposes, the approximation of the same set of data points by the "skew" Gaussian function yields $\chi^2 = 8.05 \times 10^{-7}$ cm^2. In the latter case the following set of parameters of eq 5 was obtained: $A = 0.175$, $\nu' = -26.4$ cm^{-1}, $\sigma = 6.42$ cm^{-1}, $k_1 = -0.2875$, $k_2 = 0.288$ 1/cm^{-1}.

In the final analysis, our model function was a sum of 40 Boltzmann-weighted profiles (eq 5) computed in steps of 600 cm^{-1} in E_{vib} and then convolved with rotational band profile (eq 3) and the Lorentzian component of our spread function. The only fitting parameter used in approximating the spectra measured (naturally apart from the quantity V in eq 1 used for the binding of the intensities of the spectra) was the vibrational temperature T_{vib} of the molecules. As in the case of approximation of the model profiles, we also stuck to the least-squares tenet (having replaced the quantities $M(x;\{p\})$ and $D(x)$ in eq 6 by $MS(\nu;T_{vib})$ and $ES(\nu)$, respectively, the latter standing for the experimental spectrum), but subject to the additional condition

$$\sum_i [ES(\nu_i) - MS(\nu_i;T_{vib})] = 0$$

which means the equality of the spectrum-integrated intensities.

The model spectra obtained as a result of this fitting procedure are presented in Figure 3 in the form of smooth solid curves. (The approximate value of T_{vib} indicated in the lowermost figure and also the intermittent character of the model envelope merely characterize the center of gravity of the distribution of photomeasurements for this spectrum. The exact vibrational temperature is in this case difficult to determine, first, because of the small number of the counts themselves and second, because the given data array was not bounded above as to the Φ_{IR} value in the course of signal accumulation, and so the vibrational distribution for this array may be additionally broadened.)

4. Discussion

Comparison between the experimental spectra and their theoretical counterparts (smooth solid curves in Figure 3) shows that the model quite adequately describes the spectra measured in a fairly wide temperature interval, up to $T_{vib} = 1320$ K. In the latter case, the average molecular energy $\epsilon \simeq 11\,400$ cm^{-1}, which approximately corresponds to half the dissociation energy of UF_6 ($D_0(UF_6) = 23\,800$ cm^{-1}).[20] The model used by us correctly predicts the position of the maximum, as well as the shape and width, of the Raman spectra of the mode ν_1 of highly excited UF_6 molecules. If we take the values of the energy absorbed as a result of the IR MPE of UF_6 measured in ref 14 and calculate on their basis the corresponding T_{vib} values, the latter will be in good agreement with the values obtained in this work and indicated in Figure 3. All of this allows us to conclude that the method developed in ref 8 for computing the parameters of QC $\rightarrow$ QC transitions and based on due regard for statistical inhomogeneous broadening is good for UF_6 as well. Recall that this method presupposes the dominant contribution of the SIB effect to the formation of QC $\rightarrow$ QC transition bands, compared to homogeneous broadening. The fact that good agreement exists between the experimental and theoretical spectra is apparently evidence that the contribution from homogeneous broadening in the case of the mode ν_1 of UF_6 is indeed not so great, as is also the case with SF_6. At the same time, the actual "quality" of the spectra measured does not allow us to make more definite, quantitative estimates of the contribution from the homogeneous broadening associated with the IVR processes. The pulsed "heating" of the molecules used in this work, and also in ref 9 for SF_6, features inevitable T_{vib} fluctuations from pulse to pulse. Also, some uncertainty remains as to whether the Boltzmann population distribution has had enough time to get established completely by the moment the given spectral measurement is taken. Stationary heating, despite its inherent narrower interval of possible temperatures, provides for a substantially higher temperature stability. Our measurements of the Raman spectra in the vicinity of the frequency of the mode ν_1 in SF_6 taken under stationary heating conditions[21] enabled us to estimate more accurately both the magnitude of the homogeneous broadening itself and the ratio between the contributions from the two different broadening mechanisms

to the shape of the transition band profile. To illustrate, for molecules with $E_{vib} = 10\,000$ cm^{-1}, the ratio between the parameters characterizing the width of the corresponding profiles is $\gamma_L/\sigma_0 \sim 0.5$. Apparently in the case of the mode ν_1 in UF_6 the relative contribution from homogeneous broadening to the whole width is also hardly more than some 30%. A greater contribution from homogeneous broadening would make the difference between the theoretical and experimental spectra noticeable, even with such "quality" of the latter as was attained in this work.

Statistical inhomogeneous broadening causes the QC → QC transition profile to broaden and the position of its maximum to shift substantially. As can be seen from Figure 4, for $E_{vib} = 20\,000$ cm^{-1} the position of the maximum of the transition profile is shifted by $\Delta\nu_{max}(UF_6) = -29.5$ cm^{-1} toward the "red" side from the frequency of the unperturbed Raman-active mode ν_1 in UF_6, the width of the profile $2\sigma_0(UF_6)$ being equal to 9.91 cm^{-1}. Note that for SF_6 at $E_{vib} = 20\,000$ cm^{-1}, the profile width is approximately the same, $2\sigma_0(SF_6) = 9.57$ cm^{-1}, whereas the shift is considerably greater, $\Delta\nu_{max}(SF_6) = -42.7$ cm^{-1}.[9] This is due to the fact that the values of all the anharmonic constants x_{1i} in SF_6 are substantially higher than in UF_6, and it is exactly the average value of these constants that governs the position of the transition profile maximum. The profile width $2\sigma_0$ depends on the dispersion of the anharmonic frequency shifts of transitions from states differing in the set of occupation numbers (see eq 4). The distributions of the products $x_{1i}n_i$ in SF_6 and UF_6 prove to be approximately the same (the lower values of x_{1i} in UF_6 are partially offset by the higher values of n_i for a given E_{vib}), and therefore the transition profile widths for these molecules are also closely similar. Note that the random character of the distribution of the values of the anharmonic constants x_{1i} and fundamental frequencies ν_i gives rise to the Gaussian shape of the transition profile. Too great a deviation of any parameter from the average value, as is the case with x_{12} and x_{13} in UF_6 (see the discussion of Figure 4c in section 3), may make the transition profile shape other than Gaussian.

5. Conclusions

Our investigations into highly excited XY_6-type molecules (UF_6 in this work and SF_6 and WF_6 in refs 8−11) have shown that even when these molecules are excited sufficiently high into their quasicontinua, the spectra of their vibrational transitions remain adequately structured and localized in the neighborhood of the unperturbed frequency of the mode of interest. At the same time, as the vibrational energy of these molecules is increased, these spectra broaden and shift toward the long-wavelength region. The principal contribution to the formation of the QC → QC transition profiles for the molecules under study comes from the statistical inhomogeneous broadening effect. At least for the ν_1 vibrations in UF_6 and ν_1 and ν_3 vibrations in SF_6, this conclusion has been confirmed experimentally. The method developed in ref 8 makes it possible to compute in the SIB approximation the main parameters of QC → QC transitions (the intensity, shape, and position of their profiles) on the basis of the standard spectroscopic information − the values of the fundamental frequencies ν_i and anharmonicity constants x_{ij}. The Raman spectra thus calculated for highly excited SF_6 molecules fit well their experimental counterparts.[9] We think that the agreement between the measured and calculated spectra for UF_6 obtained in the present paper is fairly good, too. In our view, the method developed can be used successfully to describe the spectra of other highly excited molecular species. Even if the contribution from homogeneous broadening is not known exactly, which is usually the case, but there are, at least, good grounds to believe that this contribution is smaller than that from inhomogeneous broadening, calculations in the SIB approximation should correctly reflect the main characteristics of the spectra of one-photon processes, such as IR fluorescence and spontaneous Raman scattering. Of course, when describing multiple-photon processes, e.g., IR MP excitation, which involve the absorption of many photons, one should take account of homogeneous broadening, especially at the edges of the spectrum, where the role of the Lorentzian wings may be decisive. One of the possible ways to find the homogeneous broadening parameters for IR transitions has been suggested in ref 10.

References and Notes

(1) *Laser Spectroscopy of Highly Vibrationally Excited Molecules*; Letokhov, V. S., Ed.; Adam Hilger: Bristol, England, 1989.
(2) Quack, M.; Kutzelnigg, W. *Ber. Bunsen-Ges. Phys. Chem.* **1995**, *99*, 231.
(3) Nesbitt, D. J.; Field, R. W. *J. Phys. Chem.* **1996**, *100*, 12735.
(4) Crim, F. F. *J. Phys. Chem.* **1996**, *100*, 12725.
(5) Moore, C. B.; Smith, I. W. M. *J. Phys. Chem.* **1996**, *100*, 12848.
(6) Lehmann, K. K.; Scoles, G.; Pate, B. H. *Annu. Rev. Phys. Chem.* **1994**, *45*, 241.
(7) Boyarkin, O. V.; Rizzo, T. R. *J. Chem. Phys.* **1995**, *103*, 1985.
(8) Makarov, A. A.; Petrova, I. Yu.; Ryabov, E. A.; Letokhov, V. S. *J. Phys. Chem. A* **1998**, *102*, 1438.
(9) Malinovsky, A. L.; Petrova, I. Yu.; Ryabov, E. A.; Makarov, A. A.; Letokhov, V. S. *J. Phys. Chem. A* **1998**, *102*, 9353.
(10) Lokhman, V. N.; Petin, A. N.; Ryabov, E. A.; Letokhov, V. S. *J. Phys. Chem. A* **1999**, *103*, 11293.
(11) Lokhman, V. N.; Makarov, A. A.; Petrova, I. Yu.; Ryabov, E. A.; Letokhov, V. S. *J. Phys. Chem. A.* **1999**, *103*, 11299.
(12) Malinovsky, A. L.; Makarov, A. A.; Ryabov, E. A.; Tishina, E. N. *Khim. Fiz.* (Chemical Physics) **1999**, *18*, 9 (in Russian).
(13) Tiee, J.; Wittig, C. *Appl. Phys. Lett.* **1977**, *30*, 420.
(14) Alimpiev, S. S.; Karlov, N. V.; Nabiev, Sh. Sh.; Nikiforov, S. H.; Prokhorov, A. M.; Sartakov, B. G. *Kvantovaya Elektronika* (Sov. Journ. of Quantum Electronics) **1981**, *8*, 623 (in Russian).
(15) Bagratashvili, V. N.; Vainer, Yu. G.; Doljikov, V. S.; Koliakov, S. F.; Makarov, A. A.; Malyavkin, L. P.; Ryabov, E. A.; Silkis ,E. G.; Titov, V. D. *Appl. Phys.* **1980**, *22*, 101.
(16) Malinovsky, A. L. Ph.D. Thesis, 1997, Institute of Spectroscopy, Russian Academy of Sciences, Troitsk, Russia.
(17) Cahen-de Villardi, J.; Clerc, M.; Isnard, P.; Weulersse, J. M. *J. Mol. Spectrosc.* **1980**, *84*, 319.
(18) Aldridge, J. P.; Brock, E. G.; Filip, H. *J. Chem. Phys.* **1985**, *83*, 34.
(19) McDowell, R. S.; Asprey, L. B.; Paine, R. T. *J. Chem. Phys.* **1974**, *61*, 3571.
(20) Becker, F. S.; Kompa, K. L. *Nuclear Technology* **1982**, *58*, 329.
(21) Blinov, P. S.; Malinovsky, A. L.; Ryabov, E. A., paper in preparation.